

Establishing a Numerical Modeling Framework for Hydrologic Engineering Analyses of Extreme Storm Events

Xiaodong Chen, S.M.ASCE¹; Faisal Hossain, A.M.ASCE²; and L. Ruby Leung³

Abstract: In this study, a numerical modeling framework for simulating extreme storm events was established using the weather research and forecasting (WRF) model. Such a framework is necessary for the derivation of engineering parameters such as probable maximum precipitation that are the cornerstone of large water-management infrastructure design. Here, this framework was built based on a heavy storm that occurred in Nashville, Tennessee (USA), in 2010, and verified using two other extreme storms. To achieve the optimal setup, several combinations of model resolutions, initial/boundary conditions (IC/BC), cloud microphysics, and cumulus parameterization schemes were evaluated using multiple metrics of precipitation characteristics. The evaluation suggests that WRF is most sensitive to the IC/BC option. Simulation generally benefits from finer resolutions up to 5 km. At the 15 km level, NCEP2 IC/BC produces better results, whereas NAM IC/BC performs best at the 5 km level. The recommended model configuration from this study is: NAM or NCEP2 IC/BC (depending on data availability), 15 km or 15 km–5 km nested grids, Morrison microphysics, and Kain-Fritsch cumulus schemes. Validation of the optimal framework suggests that these options are good starting choices for modeling extreme events similar to the test cases. This optimal framework is proposed in response to emerging engineering demands of extreme storm event forecasting and analyses for design, operations, and risk assessment of large water infrastructures. DOI: 10.1061/(ASCE)HE.1943-5584.0001523. © 2017 American Society of Civil Engineers.

Author keywords: Precipitation; Heavy storms; Nashville; Atmospheric model; Parameterizations.

19.2 Introduction

Intense storms, or extreme rainfall events, as they will be called hereafter, pose challenges to infrastructure management and design and trigger other catastrophic events such as floods, landslides, and dam failures (Casagli et al. 2006; Cong et al. 2006; Evans et al. 2000). They are also the cornerstone of engineering design and risk assessment of large infrastructures such as dams, levees, and power plants (Stratz and Hossain 2014). Therefore, it is of great societal interest to physically predict and understand the occurrence and magnitude of such extreme events for both design and operation of engineering infrastructures.

In current engineering practice, the safety of hazardous infrastructures (where lives are at stake with infrastructure failure) is achieved through designs based on probable maximum precipitation (PMP). PMP is defined as the theoretical greatest depth of precipitation for a given duration that is physically possible over a particular drainage area (Huschke 1959). It depicts the precipitation potential of an already intense storm that is maximized to an upper bound using some basic engineering assumptions (Kunkel et al. 2013; Stratz and Hossain 2014). The National Oceanic

and Atmospheric Administration (NOAA) has created a database of such intense storms in the United States from approximately 1900–1990 that were maximized to PMPs and publicly released as hydrometeorological reports (HMRs) for the engineering infrastructure community (U.S. Department of Commerce 1999). For engineering practices outside the United States, the World Meteorological Organization (WMO) has outlined several approaches that can be used (WMO 1986). In general, these are local methods (maximization of local storms), transposition methods (storm transposition from same climatological regions), generalized methods (based on some provided PMP distribution maps), and statistical methods such as the one proposed in Hershfield (1965).

PMP is generally expressed mathematically as: $P \times w_{p(\text{maximum})}/w_{p(\text{storm})}$, where P = the observed rainfall accumulation; $w_{p(\text{maximum})}$ = the highest observed precipitable water from historical records; and $w_{p(\text{storm})}$ = the storm precipitable water. This approach is often criticized as being insufficiently physical because it assumes a linear relationship between precipitation and the water-holding capacity of the atmosphere (Abbs 1999; Kunkel et al. 2013). Also, it heavily relies on historical observation data. For very early extreme events used in PMP analysis (such as Storm Elba of 1929), it is difficult to obtain a physically consistent picture because of limitations of record keeping and the linearity assumption (Abbs 1999). In this context, numerical simulation of extreme storms and their consequent physical maximization to a PMP is gaining much more traction among science and engineering communities than before (Kunkel et al. 2013; Stratz and Hossain 2014).

The numerical modeling approach has several key advantages over the traditional approaches. It is able to produce finer details on the spatial-temporal structure of the storms using fewer assumptions and experience-based estimation. It is more tailored to a region that has little or no long-term rainfall record or is rapidly

¹Graduate Student, Dept. of Civil and Environmental Engineering, Univ. of Washington, More Hall 201, Seattle, WA 98195.

²Associate Professor, Dept. of Civil and Environmental Engineering, Univ. of Washington, More Hall 201, Seattle, WA 98195 (corresponding author). E-mail: fhossain@uw.edu

³Laboratory Fellow, Atmospheric Sciences and Global Change Division, Pacific Northwest National Laboratory, 902 Battelle Boulevard, Richland, WA 99352.

Note. This manuscript was submitted on June 4, 2016; approved on January 19, 2017. **No Epub Date.** Discussion period open until 0, 0; separate discussions must be submitted for individual papers. This paper is part of the *Journal of Hydrologic Engineering*, © ASCE, ISSN 1084-0699.

73 undergoing changes in weather patterns due to land cover change or
 74 global warming. More importantly, a well-established numerical
 75 modeling framework is often able to handle various extreme events
 76 within the model domain spanning decades (Chen and Hossain
 77 2016). In the study by Tan (2010), the WRF model was calibrated and
 78 and set up over the American River basin. It was found capable of
 79 simulating various PMP-class storms in the basin during 1970–
 80 2000. The model also provided better space-time pictures of
 81 the historical events that were used in HMRs for PMP estimation
 82 in this basin. This is another benefit of the numerical modeling
 83 approach.

84 There have been numerous studies on extreme events or PMPs
 85 using numerical atmospheric models. Some conclusions have been
 86 reached on the optimal setup of numerical models. For example,
 87 optimal grid size ratios of 1:7, 1:5, and 1:3 were validated over
 88 eight storms in southwest England (Liu et al. 2012). The study
 89 by Pennelly et al. (2014) concluded that for storms in Alberta,
 90 Canada, 6-km grids in the WRF model are a balance between sim-
 91 ulation quality and time expense. There have also been efforts to
 92 optimize the simulated rainfall results by operating models with
 93 more information. For example, Giannaros et al. (2016) assimilated
 94 lightning data into the atmospheric numerical simulation, and it
 95 helped improve precipitation forecast. However, a consistent
 96 framework informing the users from the hydrologic engineering
 97 community how to systematically set up and analyze numerical
 98 models for engineering analyses is still absent from the literature.

99 Previous studies suggest that the performance of storm simula-
 100 tion heavily depends on the parameterization schemes, which is the
 101 mathematical identification of physical processes in the numerical
 102 models (Stensrud 2009). Though a wise choice of parameterization
 103 schemes results in improved simulations of big storms, it often has
 104 to be achieved by trial and error. For example, several numerical
 105 studies for the Mumbai July 2005 storm (Chang et al. 2009; Kumar
 106 et al. 2008; Rao et al. 2007; Vaidya and Kulkarni 2007) show
 107 steady progress in reconstructing the high precipitation values in
 108 the various modeling platforms with different parameterization
 109 schemes. Rajeevan et al. (2010) revealed that the optimal combi-
 110 nations of parameterization schemes and IC/BC in the model can be
 111 quite different for southeast Indian thunderstorms. These high
 112 heterogeneities within optimal model configurations make it diffi-
 113 cult for engineering communities to set up and operate these
 114 models.

115 Given that the engineering community is relatively new to the
 116 setup and operation of numerical models, as well as the use of mod-
 117 els for maximization of extreme storms in PMP estimation, a frame-
 118 work to explore the role of various parametrizations and IC/BC
 119 on extreme storm simulation accuracy can provide a baseline for
 120 optimal criteria for PMP simulation. Such a comprehensive study
 121 will also illustrate ways to identify optimal model configurations
 122 for extreme storm simulations and help the engineering infrastruc-
 123 ture community that engages in hydrologic analyses for design and
 124 operations embrace numerical models for PMP estimation and fur-
 125 ther advance the methodology.

126 In this study, ways to establish a generic numerical modeling
 127 framework over a given area are investigated. Taking the Nashville,
 128 Tennessee, USA, 2010 storm as a test case, the procedures required
 129 to achieve a good storm reconstruction using the WRF model
 130 are illustrated. Various combinations of parameterization schemes,
 131 IC/BCs, and grid sizes are evaluated. Using this framework, three
 132 questions are addressed:

- 133 1. What combinations of model options in WRF are most skillful
- 134 for extreme storm event simulation?
- 135 2. What are the strengths and weaknesses of each model option in
- 136 reference to simulation accuracy of extreme precipitation?

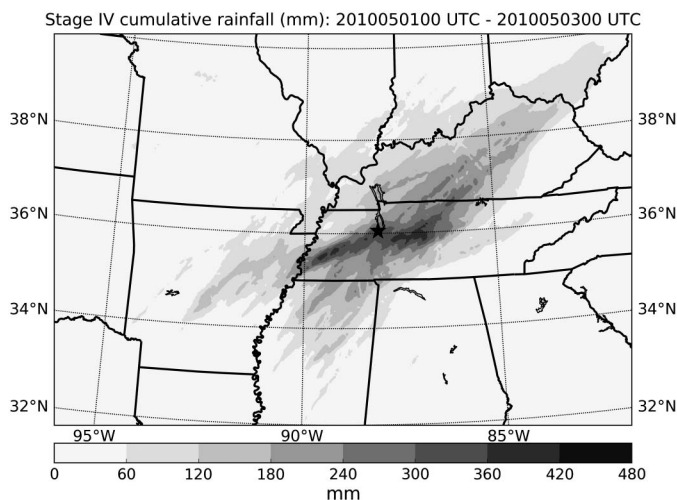


Fig. 1. 48-h (0000 UTC 1 May–0000 UTC 3 May, 2010) total rainfall from Stage IV data

3. What are the optimal model configurations for engineering operations and infrastructure implications?

Nashville, USA 2010 Extreme Storm

During May 1 and May 2, 2010, the west and middle Tennessee region of the USA experienced a record-breaking storm. This 2-day rainfall event brought huge amounts of water to western Tennessee, with 48-h cumulative rainfall exceeding historical records at several gauge stations (such as the Nashville and Camden station in Tennessee). Fig. 1 shows the 48-h cumulative rainfall from this storm as observed from the NEXRAD network, which shows a southwest–northeast pattern.

This storm, hereafter referred to as the Nashville 2010 storm, led to a flood in the following days that NOAA categorized as a 1000-year return period flood event (NOAA National Weather Service and Weather Forecast Office, NWSWF 2010). The maximum 48-h total precipitation observed was 493 mm (19.41 in.) at the Camden COOP station (36.05°N, 88.08°W, the star in Fig. 1). This value is quite close to the 5,000 mi² 48-h design PMP (495 mm, or 19.5 in.) for west Tennessee (an area in the HMR 1951 report, hereafter referred to as the HMR51 region). Nashville’s international airport recorded its first and third highest 24-h total rainfall in history on 1 and 2 May, respectively (NWSWF 2010). These statistics qualify this rainfall event as a reference extreme storm for PMP design for the HMR 51 region. During the ensuing flood event, 21 deaths were reported, and over 30 counties were declared major disaster areas by the government. This unique rainfall record and infrastructure-damaging impact make this event worth revisiting with numerical simulation (Durkee et al. 2012). There have not been many numerical simulation efforts on this storm. Thus, a successful model reconstruction of this event would provide an important baseline for studying other local events or events in similar environmental conditions for engineering infrastructure applications.

The Nashville 2010 storm was among a series of big storms (tornados 41, 43, and 57) hitting the mid-southern United States in the same period. Analysis of reanalysis products suggests that the event was associated with a synoptic system with significant atmospheric moisture. The Atlantic ridging associated with the negative phase of the North Atlantic Oscillation (NAO) helped

176 amplify and slow the eastward propagating synoptic wave pattern
 177 that generated heavy precipitation from mesoscale organized con-
 178 vective systems (Durkee et al. 2012). An atmospheric river origi-
 179 nating from the Intertropical Convergence Zone (ITCZ) in Central
 180 America provided the moisture source for this record-breaking
 181 event (Durkee et al. 2012). Surface topography in the Appalachians
 182 provided orographic forcing for moisture convergence, and land
 183 surface heating helped maintain atmospheric instability, so precipi-
 184 tation continued until 2 May, 2010. Previous studies have identified
 185 several key atmospheric factors such as the superposition of the
 186 polar and subtropical jet (Winters and Martin 2014) and the atmo-
 187 spheric river (Durkee et al. 2012; Moore et al. 2012). Because some
 188 elements present in the Nashville 2010 event are common ingredi-
 189 ents in other extreme storms, reconstructing this extreme event
 190 may serve as an important test case for evaluating the ability of
 191 the WRF model for simulating other storms.

192 The Numerical Atmospheric Model

193 The WRF model is employed for big storm reconstruction. WRF
 194 is an atmospheric modeling system (Skamarock et al. 2008) that
 195 features two nonhydrostatic solvers, the advanced research WRF
 196 (ARW) core for atmospheric research, and the nonhydrostatic meso-
 197 scale model (NMM) core for the operational forecast. This study
 198 adopted WRF-ARW v3.6.1 for the storm simulation. WRF-ARW
 199 has been employed in various big storm studies and demonstrated
 200 to be capable of simulating several big storms across the world
 201 (Chen and Hossain 2016; Kumar et al. 2008; Rajeevan et al.
 202 2010; Tan 2010).

203 WRF-ARW is designed for mesoscale meteorological simula-
 204 tion with spatial resolution ranging from 1 to 100 km. Accordingly,
 205 the time step used in the model varies from seconds to minutes. It
 206 simulates atmospheric motion using compressible, nonhydrostatic
 207 Euler equations with consideration of mass, energy, and momen-
 208 tum conservation. These equations are formulated and solved using
 209 the Arakawa-C grid with terrain-following mass vertical coordi-
 210 nates (Laprise 1992). WRF-ARW uses various parameterization

211 schemes to estimate the atmospheric processes at the subgrid scale,
 212 and atmospheric moisture is considered in various phases in the
 213 cloud microphysics parameterization schemes. For example, in
 214 the Morrison microphysics scheme, water is considered in vapor,
 215 cloud droplets, cloud ice, rain, snow, and graupel or hail phases
 216 (Morrison et al. 2009). This ensures an accurate description of
 217 moisture in the air. By default, the WRF-ARW model uses the
 218 USGS or MODIS land use dataset to depict the surface feedback.
 219 As a platform, the WRF-ARW model provides multiple choices for
 220 major physics processes that affect the atmospheric state: cloud mi-
 221 crophysics, cumulus processes, radiation processes, planetary
 222 boundary layer processes, and land surface processes. With this
 223 modular design, it exhibits great flexibility for mesoscale atmo-
 224 spheric activities across a wide range of temporal and spatial scales
 225 while maintaining the capability of incorporating recent advances
 226 in atmospheric sciences.

Experimental Design

228 Previous studies suggest that the performance of numerical atmo-
 229 spheric models is mostly affected by cloud physics parameteriza-
 230 tion, model resolution, and initial and boundary conditions in
 231 the model, as well as the simulation period. The subsequent steps
 232 illustrate the workflow needed by engineers to establish the optimal
 233 modeling framework based on WRF. A schematic is shown in
 234 Fig. 2, and the details of each step are explained subsequently with
 235 an example of the Nashville 2010 storm simulation.

- 236 1. Study previous modeling efforts to understand the background
 237 of the study domain;
- 238 2. Determine the atmospheric numerical model(s) of interest;
- 239 3. Determine the study domain and simulation period. Prioritize
 240 the main physical factors in the model that affect the simulation
 241 quality. This can be gained from step 1. Outline the model op-
 242 tions (i.e., combination of parameterizations) to be tested;
- 243 4. Collect the input data, set up the model, and make model runs;
- 244 5. Determine the main purpose of the modeling framework and the
 245 evaluation criteria. As shown subsequently in the Nashville

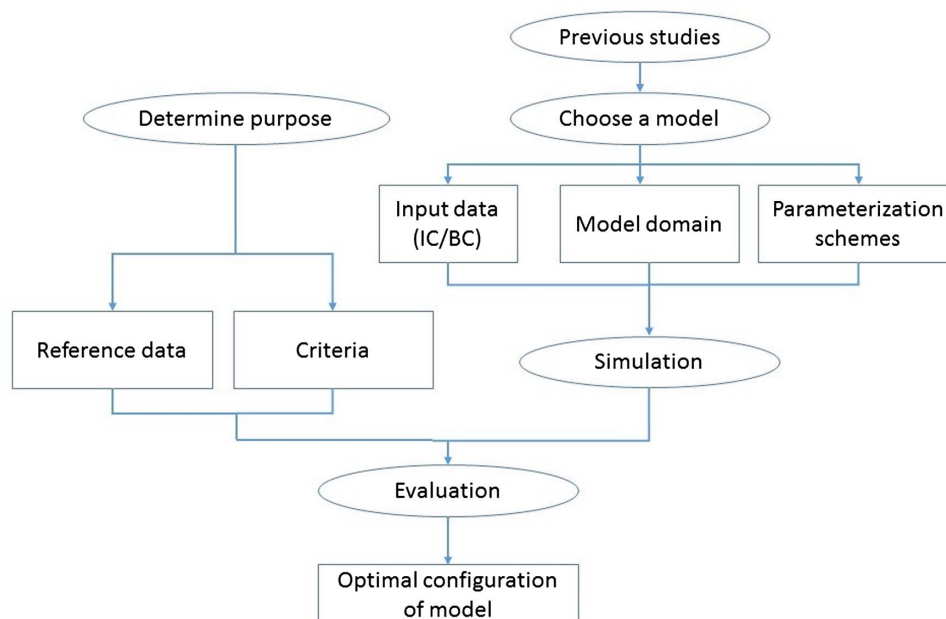
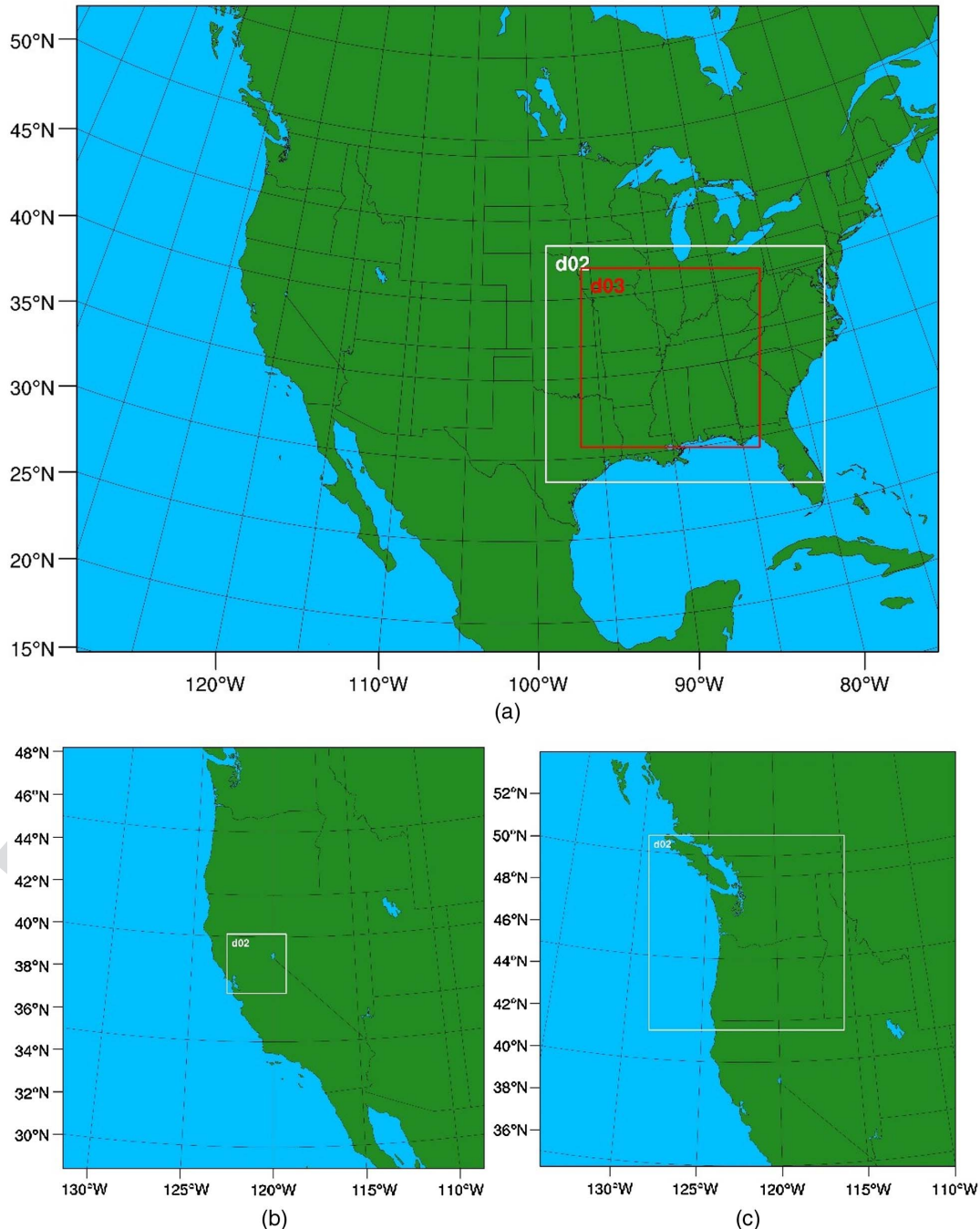


Fig. 2. Generic framework for exploring optimal model configuration for extreme storms

246 2010 case, different purposes of the modeling framework re- 260
 247 quire different criteria and lead to different configurations in 261
 248 the optimal atmospheric model. Collect the reference data; 262
 249 6. Evaluate the simulation results using the metric(s) that best 263
 250 serve the purpose. 264
 251 The Nashville 2010 storm period is May 1–2, 2010, and pre- 265
 252 vious studies (Mahoney 2013) concluded that a long spin-up would 266
 253 result in less rainfall during the event. Thus, the simulation period is 267
 254 chosen as 0000 UTC 1–3 May 2010. Here, three configurations of 268
 255 nested domains were tested to evaluate model performance at 15-, 269
 256 5-, and 1.6-km (the latter is referred to as “2 km” for convenience) 270
 257 grid sizes. Fig. 3 shows the domains in the simulation of the 271
 258 Nashville 2010 storm and two verification events (which will be 272
 259 discussed later). The three nested domains in Fig. 3(a) are all 273

centered over western Tennessee. In the first configuration [g15, 260
 the outmost domain in Fig. 3(a)], the domain covers the contiguous 261
 US at 15-km grid spacing. In the second configuration [g5, the 262
 whole domain plus the white box in Fig. 3(a)], a d02 domain at 263
 5-km resolution (white box) is nested inside the larger 15-km do- 264
 main. The third configuration [g2, Fig. 3(a)] further includes a d03 265
 domain of 1.6-km spatial resolution (red box) to better resolve con- 266
 vection at 1.6-km grid spacing. When there is more than one do- 267
 main involved in the simulation, WRF runs in a two-way nesting 268
 mode, which means the coarse grid results are updated using results 269
 in finer grids where available. This experiment design allows evalu- 270
 ation of the impacts of higher resolution achieved through nesting 271
 with the same placement of the outermost lateral boundaries for all 272
 simulations. Nominal time steps of 60, 20, and 6.7 s were used for 273



F3:1

Fig. 3. Spatial domain in modeling framework of Nashville 2010 storm, 1997CA event and 1980PNW event

274 the 15-, 5-, and 1.6-km grids, respectively. Model outputs are ar- 306
 275 chived hourly between 0000 UTC 1 May 2010 and 0000 UTC 3 307
 276 May 2010, similar to Moore et al. (2012).

277 Three sources of data were used to generate IC/BCs: (1) NCEP/ 308
 278 DOE reanalysis product (NCEP2) at 2.5-degree resolution; 309
 279 (2) NCEP/NCAR reanalysis product (NNRP) at T62 (209-km) res- 310
 280 olution; and (3) North America mesoscale (NAM) forecast output at 311
 281 T221 (32-km) resolution. For this study, the NAM forecast initial-
 282 ized at 0000 UTC 1 May 2010 was used.

283 Previous studies suggest that precipitation simulation is more 313
 284 sensitive to microphysics and cumulus parameterization schemes 314
 285 than parameterizations for other processes in the model (Del Genio 315
 286 et al. 2005; Pennelly et al. 2014; Zhang and McFarlane 1995). 316
 287 Here, three microphysics parameterization schemes for mixed 317
 288 phase clouds were tested, including (1) Morrison double moment 318
 289 scheme (coded as “Morrison” here), (2) New Thompson scheme 319
 290 (“Thompson”), and (3) WSM-5 scheme (“WSM5”). Three cumu- 320
 291 lus parameterization schemes were also evaluated, including the 321
 292 (1) Kain-Fritsch scheme (coded as “KF” here), (2) Grell-Devenyi 322
 293 scheme (“GD”), and (3) Grell-Freitas scheme (“GF”). In the nested 323
 294 runs (g5 and g2), the cumulus scheme is used only in the 15-km 324
 295 domain because convection is explicitly resolved at the 5- and 2-km 325
 296 resolutions. Grell and Freitas (2014) noted that at coarser resolu- 326
 297 tions, the GF scheme functions as a cumulus parameterization to 327
 298 represent the unresolved deep convection, but at this solution of 328
 299 a few kilometers, deep convection is explicitly resolved and the 329
 300 GF scheme mainly represents shallow convection. Thus, another 330
 301 set of simulations are designed to test the scale-aware GF scheme 331
 302 in which the GF cumulus scheme is applied to all the domains 332
 303 (15 km, 5 km, 2 km) in the nested runs (g5 and g2). Other schemes 333
 304 are fixed in all the experiments, and they are: RRTM long wave 334
 305 radiation scheme, Dudhia shortwave radiation scheme, revised

MM5 surface layer scheme, Yonsei University (YSU) planetary 306
 boundary layer scheme, Noah land surface scheme. 307

The total number of combinations of the different options in grid 308
 sizes (3), IC/BCs (3), microphysics schemes (3), and cumulus 309
 schemes (3 in the g15 runs, 2 in the g5 and g2 runs) amounts 310
 to 63 WRF runs designed and conducted for this study. 311

Framework Evaluation Metrics 312

Independent precipitation observation data are required for the 313
 assessment of the storm simulations. One option is gauge data 314
 because they provide the most accurate estimate of rainfall amount 315
 and duration. In some cases, gauge data may not be available due to 316
 either the age of the storm or the gauges having stopped working 317
 (such as the Nashville international airport station in the Nashville 318
 2010 storm event); the gridded data can be used to validate model 319
 results. Here, the NEXRAD Stage IV precipitation dataset (Fig. 1) 320
 is used as the reference in selecting the optimal model configura- 321
 tion, given its high accuracy and good spatial coverage. Cumulative 322
 48-h rainfall is evaluated by the spatial correlation coefficient be- 323
 tween the simulated and Stage IV 48-h total rainfall. This reveals 324
 how the model performs in capturing the rainy area and the spatial 325
 heterogeneity of total rainfall. For extreme rainfall events used in 326
 engineering analysis, it is important that the numerical model cap- 327
 ture the core precipitating areas as accurately as possible. The val- 328
 idation steps used the Livneh daily CONUS near-surface gridded 329
 meteorological data (Livneh et al. 2013). This dataset is developed 330
 from gauge observations, and it provides an estimation of daily pre- 331
 cipitation. By validating the results using a different reference, 332
 reference-dependent conclusions can be avoided. 333

Additional metrics employed include: probability of detection 334
 (POD), false alert ratio (FAR), frequency bias (Bias), Heidke skill 335
 score (HSS), critical success index (CSI, or TS), and Gilbert skill 336
 score (GSS, or ETS). They are defined as statistics of the binary 337
 result indices in Table 1. Table 2 shows the definitions of these 338
 metrics, as well as the ranges of their values. These metrics measure 339
 only the accuracy in the coverage of the rainy versus nonrainy area. 340
 Therefore, when the magnitude of precipitated water matters a lot, 341
 it would be better to use the correlation or root mean square error 342
 (RMSE) between observed rainfall and simulated rainfall for the 343
 period of interest (e.g., 6, 24, 48, and 72 h in the PMP design). 344

Table 1. Binary Results Indices for Spatial Coverage Evaluation Metric

T1:2	Simulated	Observed		Sum
		Yes	No	
T1:3	Yes	Hits (<i>YY</i>)	False alarms (<i>YN</i>)	<i>YY + YN</i>
T1:4	No	Misses (<i>NY</i>)	Correct rejections (<i>NN</i>)	<i>NY + NN</i>
T1:5	Sum	<i>YY + NY</i>	<i>YN + NN</i>	Total = <i>YY + YN</i> + <i>NY + NN</i>

Table 2. Definition of Evaluation Metrics on Storm Performance in Spatial Coverage Using Metrics from Table 1

T2:1	Metric	Definition	Best score	Worst score
T2:2	POD	$\frac{YY}{YY + NY}$	1	0
T2:3	FAR	$\frac{YN}{YY + YN}$	0	1
T2:4	Bias	$\frac{YY + YN}{YY + NY}$	1	0 or ∞
T2:5	HSS	$\frac{2 \times (YY \cdot NN - YN \cdot NY)}{(YY + NY)(NY + NN) + (YY + YN)(YN + NN)}$	1	$-\infty$
T2:6	TS	$\frac{YY}{YY + NY + YN}$	1	0
T2:7	ETS	$\frac{YY - YY_{rand}}{YY + NY + YN - YY_{rand}}$, where $YY_{rand} = \frac{(YY + YN)(YY + NY)}{Total}$	1	-1/3

Note: *YY* (hits) means both simulation and observation indicate rainfall at the grid or station; *YN* (false alarm) means only simulation indicates rainfall at the grid/station; *NY* (misses) means only observation indicates rainfall at the grid or station; *NN* (correct rejection) means neither observation nor simulation indicates rainfall at the grid or station. More details are in Table 1. All these metrics are monotonous, except for bias.

345 This can be done using either station data or gridded data. Other
 346 terms worth considering are the storm duration (start time and end
 347 time) and peak rainfall (to classify the storm severity). The Nash-
 348 Sutcliffe model efficiency coefficient (NS) is also used to quantify
 349 the simulated precipitation. When applied to a map, this coefficient
 350 can be defined by Eq. (1), where N = the total number of grid points
 351 in the map; P_o = the observed precipitation; and P_m is the simulated
 352 precipitation. The range of NS is from $-\infty$ to 1, and 1 is a perfect
 353 score. A higher NS indicates stronger capacity of the model. These
 354 metrics quantitatively evaluate the model performance; thus, the
 355 recommendations given by these metrics can be applied to engi-
 356 neering practice with confidence (Bennett et al. 2013)

$$NS = 1 - \frac{\sum_{n=1}^N (P_o^n - P_m^n)^2}{\sum_{n=1}^N (P_o^n - \bar{P}_o)^2} \quad (1)$$

357 These metrics measure different aspects of model performance
 358 and provide different recommendations for the best combination of
 359 parameterizations to support different applications. The POD met-
 360 ric and storm duration are more useful if the successful forecast of
 361 the rainy area is more important, such as the search for possible
 362 shelter areas. The FAR metric should be weighted more if the cost
 363 of emergency relocation is high, in which case unnecessary effort
 364 related to areas that are actually not rainy should be avoided. In the
 365 infrastructure design practice, the total amount of rainfall and peak
 366 rainfall would be more important. If simulated rainfall data is being
 367 used as input to other models (such as hydrological models for
 368 stream flow forecasting), then a high spatial correlation or Nash-
 369 Sutcliffe coefficient between simulated and observed rainfall would
 370 be more desired.

371 This paper takes multiple metrics into consideration as a set
 372 when assessing model performance because no single metric cap-
 373 tures all the pertinent performance features. For example, a good

374 numerical model configuration should produce a high probability
 375 of detection for rain as well as a high critical success index, but a
 376 low false alert ratio. Several metrics were combined and a unified
 377 score (US) created. The US is defined by Eq. (2), in which POD_n ,
 378 FAR_n and CSI_n are normalized metrics defined by Eqs. (3)–(5). By
 379 combining different aspects of model performance into the score,
 380 the unified score is used to identify the best combinations for the
 381 overall performance reflected by the multidimensional metrics that
 382 appeal to the engineering infrastructure community (Sikder and
 383 Hossain 2016)

$$US = POD_n^2 - FAR_n^2 + CSI_n^2 \quad (2)$$

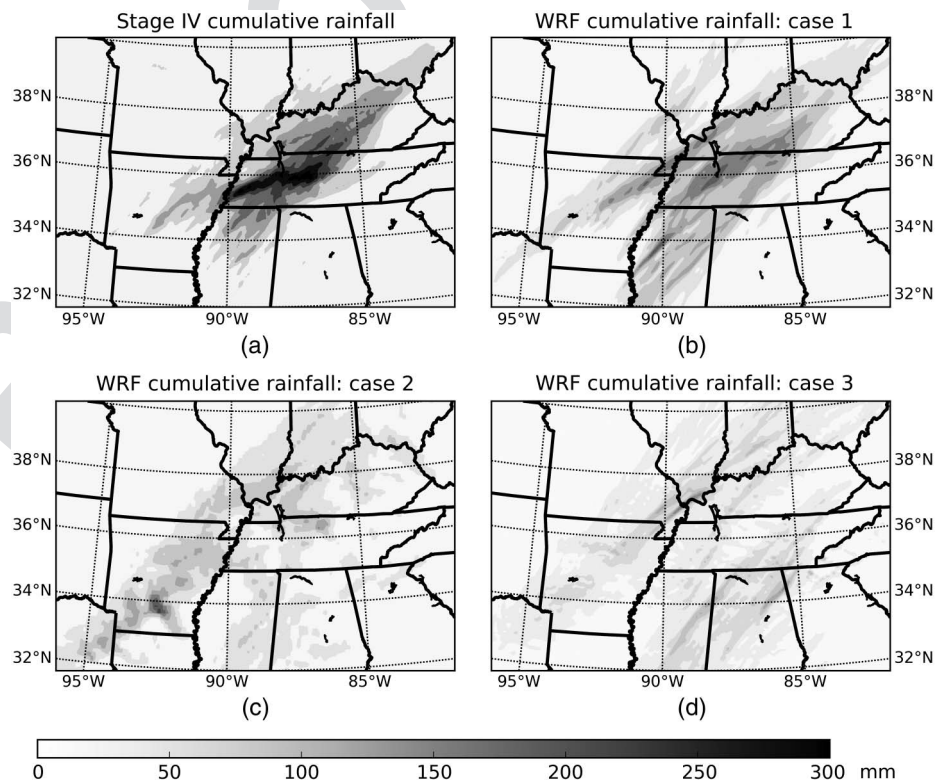
$$POD_n = \frac{POD - \min(POD)}{\max(POD) - \min(POD)} \quad (3)$$

$$FAR_n = \frac{FAR - \min(FAR)}{\max(FAR) - \min(FAR)} \quad (4)$$

$$CSI_n = \frac{CSI - \min(CSI)}{\max(CSI) - \min(CSI)} \quad (5)$$

Evaluation of Reconstruction of the Nashville 2010 Extreme Storm

384 Fig. 4 shows the observed and simulated 48-h total rainfall between
 385 UTC 0000 1 May 2010 and UTC 0000 3 May 2010. Panel 4(a)
 386 is the NEXRAD observation; panel 4(b) is from the WRF simu-
 387 lation using the g5 grids (15 km–5 km nested grids), NAM
 388 IC/BC, Morrison microphysics, and KF cumulus parameterization
 389 schemes. This is one of the best simulations suggested by the
 390
 391



F4:1 **Fig. 4.** Stage IV observed and WRF simulated 48-h (0000 UTC 1 May–0000 UTC 3 May, 2010 total rainfall during Nashville 2010 storm event

Table 3. Evaluation of Averaged 48-h Total Rainfall Simulated in the Evaluation Area (Normalized Using Stage IV Observed 48-h Total) in the Nashville 2010 Storm Event

MP	NCEP2			NNRP			NAM		
	KF	GD	GF	KF	GD	GF	KF	GD	GF
15-km grids									
Morrison	0.857	0.727	0.708	0.745	0.662	0.661	0.855	0.678	0.684
Thompson	0.921	0.774	0.744	0.797	0.711	0.707	0.879	0.719	0.719
WSM-5	0.866	0.754	0.740	0.753	0.705	0.698	0.855	0.712	0.718
5-km grids									
Morrison	0.874	—	0.766	0.695	—	0.680	0.890	—	0.759
Thompson	0.856	—	0.766	0.676	—	0.707	0.905	—	0.766
WSM-5	0.892	—	0.787	0.707	—	0.706	0.899	—	0.793
2-km grids									
Morrison	0.827	—	0.780	0.692	—	0.663	0.882	—	0.816
Thompson	0.773	—	0.723	0.636	—	0.603	0.855	—	0.781
WSM-5	0.841	—	0.794	0.683	—	0.648	0.898	—	0.829

Note: Bold numbers are the top three scores with the best performance within each grid resolution.

evaluation. Comparison of panel4(b) with panel 4(a) indicates that this model setup is able to reconstruct the heavy rainfall area in midwest Tennessee. The rainfall amount gradient is properly described by this model setup. Also, the big southwest–northeast pattern of the 48-h total rainfall is clearly captured. Panel 4(c) shows a simulation with moderate scores under evaluation, and panel 4(d) shows one of the worst simulations. Though all the simulations captured the northeast–southwest–oriented rain band, the detailed rainfall distributions from various model configurations differ a lot; thus, evaluation based on the purpose of the modeling framework is necessary. The detailed evaluation is shown as a demo of using different metrics to establish the extreme storm events modeling framework.

The Stage IV data and simulation results were all conservatively regridded to the 1/16-degree grids within the d03 domain for the following analysis. All the metrics were computed using the results within the box of lat (31°N, 40°N), lon (95°W, 84°W), which is referred to here as “evaluation area.”

The total rainfall amount in the event reveals the potential magnitude of the successive flood and suggests how destructive the storm would be. To evaluate the WRF simulated results, the ratios of simulated total rainfall to the Stage IV total rainfall over the evaluation area were calculated and shown in Table 3. Numbers

in this table are all normalized using the observed Stage IV 48-h total rainfall; thus, the closer to 1, the more accurately the model reconstructs this event. For each grid size, the top three combinations are highlighted in bold in the table.

All these combinations tend to underestimate the total rainfall in the evaluation area. However, the best results (such as g15-NCEP2-Thompson-KF and g5-NAM-Thompson-KF) are fairly close to the observed amount, with the difference within 10%. Also, the performance of NCEP2 is comparable to those of NAM IC/BC, both of which are significantly better than NNRP IC/BC. The simulated total rainfall amount is sensitive to the cumulus scheme because the difference in KF results from NCEP2 and NAM IC/BC is less than 7%, whereas the difference due to cumulus schemes is larger than 10%. The best results come from coarser resolutions. Thus, for total rainfall estimation, the optimal framework would go up to only 5 km resolution.

Table 4 shows the spatial correlations and RMSEs between the simulated 48-h total rainfall maps and the Stage IV total rainfall map. Values in parentheses are the RMSE results. For each grid size, the top three combinations in the correlation coefficient are highlighted in bold in the table. Similarly, the top three combinations in RMSE are also bolded in the table, and they are exactly those deriving the best spatial correlation. At all three grid scales,

Table 4. Spatial Correlation and RMSE between Simulated and Stage IV Reference 48-h Cumulative Rainfall Distribution in the Nashville 2010 Storm Event

MP	NCEP2			NNRP			NAM		
	KF	GD	GF	KF	GD	GF	KF	GD	GF
15-km grids									
Morrison	0.364 (65.0)	0.344 (66.4)	0.231 (69.4)	0.259 (69.4)	0.345 (66.8)	0.139 (71.6)	0.597 (55.4)	0.488 (62.2)	0.471 (62.7)
Thompson	0.359 (65.5)	0.368 (65.2)	0.254 (68.4)	0.249 (69.8)	0.344 (66.2)	0.125 (71.6)	0.606 (54.7)	0.516 (60.5)	0.516 (60.5)
WSM-5	0.365 (64.9)	0.362 (65.6)	0.271 (68.1)	0.261 (69.4)	0.361 (65.8)	0.122 (71.8)	0.589 (55.8)	0.485 (61.8)	0.418 (64.2)
5-km grids									
Morrison	0.455 (62.1)	—	0.171 (71.3)	0.311 (69.1)	—	0.154 (71.1)	0.773 (43.8)	—	0.500 (60.6)
Thompson	0.335 (68.1)	—	0.216 (69.4)	0.334 (68.5)	—	0.159 (70.7)	0.698 (49.2)	—	0.509 (60.2)
WSM-5	0.322 (68.9)	—	0.220 (70.0)	0.337 (68.0)	—	0.172 (70.3)	0.700 (49.2)	—	0.537 (58.7)
2-km grids									
Morrison	0.596 (55.6)	—	0.527 (59.3)	0.289 (70.1)	—	0.293 (70.2)	0.766 (44.4)	—	0.705 (49.4)
Thompson	0.490 (61.0)	—	0.380 (65.8)	0.277 (70.1)	—	0.302 (69.3)	0.697 (49.6)	—	0.644 (53.6)
WSM-5	0.482 (61.4)	—	0.435 (63.8)	0.318 (68.4)	—	0.313 (68.7)	0.708 (48.8)	—	0.623 (54.6)

Note: Values in parentheses are RMSE (unit: mm/day). Bold numbers are the top three scores with the best performance (highest correlation or lowest RMSE) within each grid resolution.

438 NAM provides the best estimates of the 48-h total rainfall. Within
 439 each IC/BC category, the difference from different microphysics
 440 schemes is not huge (usually only within 20% of the score), but
 441 different cumulus parameterization schemes have significant im-
 442 pacts on the precipitation simulation quality. This is especially
 443 notable in the simulations driven by the NCEP2 IC/BC, where the
 444 spatial correlation ranges from ~ 0.2 (GF scheme) to ~ 0.6 (KF
 445 scheme), and the correlations with the KF scheme are always higher
 446 than those with the GF scheme. Also, the g5-NAM-Morrison-KF
 447 case [Fig. 4(b)] produced the best spatial correlation among all
 448 the tested cases. Based on Table 3, NAM IC/BC and the KF cumu-
 449 lus scheme are recommended for storm reconstructions that address
 450 the spatial distribution of the cumulative rainfall (such as PMP de-
 451 sign). However, because this result is based only on the cumulative
 452 rainfall, it does not reveal temporal evolution information.

453 At the 5- and 2-km grid scales, all the combinations produce
 454 stronger correlations. As can be seen in the following analysis,
 455 NAM often produces the best quantitative evaluation values in
 456 the finer grids. The top combinations for the 5- and 2-km grids
 457 are similar. The difference among the best correlation results at
 458 the three different grid scales is not significant. In general,
 459 higher-resolution simulations are able to capture finer-scale fea-
 460 tures, although the improvement from 5 to 2 km is marginal.

461 In certain types of engineering infrastructure analyses, it is
 462 important to know both the location and period of the storm event.
 463 A better picture of the spatial-temporal structure of the storm

would help make better operation plans for the drainage systems,
 for example. To better evaluate the simulated spatial-temporal
 structures of the storm, quantitative scores were computed for
 the 63 simulations. Unlike the calculation of spatial correlation us-
 ing rainfall total, the computation here used hourly rainfall data.
 Fig. 5 visualizes the evaluation on the spatial coverage of hourly
 rainfall simulated by WRF. Blank panels mean the corresponding
 combination was not tested (similar to “-” in Table 3). Fig. 5(a)
 shows the POD, with greater values representing more skillful
 simulations. Similarly, Fig. 5(b) shows the FAR (lower values
 are better). POD reflects the probability of rainfall grid points being
 successfully simulated as “rainy” by the numerical model. FAR
 evaluates the simulation accuracy of nonrainy regions, so combin-
 ing it with POD can provide a better assessment of the simula-
 tion quality.

The general information from Figs. 5(a) and 5(b) suggests that
 as the numerical model takes advantage of the finer grids, the simu-
 lation quality usually improves. The g15 grid shows somewhat
 better POD than some of the g5 and g2 results, which is possible
 because POD measures only how completely the observed rainfall
 area is covered by the simulation. Fig. 5(a) suggests that the
 Morrison microphysics scheme tends to overestimate rainfall cov-
 erage, and this is supported by the higher FAR values in Fig. 5(b).
 Compared with the g15 grid, finer grid simulations are able to re-
 duce the likelihood of false alert: The range of the best three FAR
 scores in the g15 grid is [0.571, 0.588], which is less skillful than

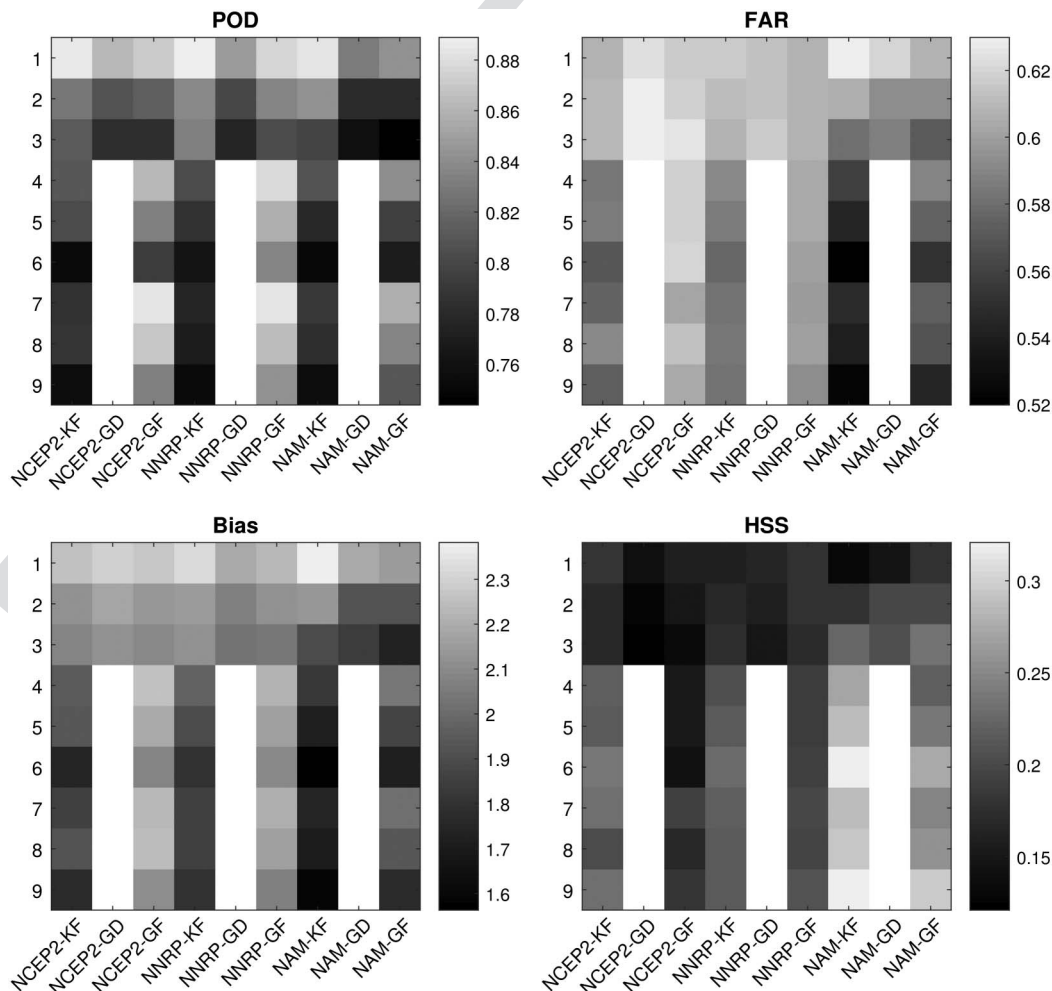


Fig. 5. Evaluation of spatial coverage simulated by WRF

490 the g5 results of [0.520, 0.551]. Similar to the findings from the
 491 spatial correlation and total rainfall analyses, the biggest difference
 492 in the FAR comes from the choice of IC/BCs: NAM outperforms
 493 others at both coarser and finer grids. Also, the WSM-5 scheme
 494 tends to produce less spatial extent of rainfall, so it performs better
 495 for the FAR score.

496 Fig. 5(c) shows the frequency bias scores. A bias score higher
 497 than 1 means the model overestimates the rainfall coverage, and a
 498 score less than 1 suggests an underestimation. As WRF is applied
 499 in the finer grids, the bias scores steadily converge to 1. All micro-
 500 physics schemes benefit from the use of the finer grids. All of the
 501 bias scores are larger than 1, which indicates that all models over-
 502 estimate the rainfall area. Because the total rainfall amount analysis
 503 suggests that all models underestimate the total rainfall amount, the
 504 simulated picture is most likely to be an expanded rainy area with
 505 a rain rate smaller than the observed rate. This is confirmed by
 506 comparing Fig. 4(b) to Fig. 4(a). Fig. 5(d) presents the HSS, with
 507 higher scores indicating better simulations. For a simulation with
 508 nonzero capability in forecasting and simulation, the HSS must be
 509 greater than 0. Fig. 5(d) shows that all 63 simulations have some
 510 capabilities for forecasting/simulation. Similar to the FAR scores,
 511 NAM IC/BC performs best at both coarser and finer grids.

The improvement from the g15 to g5 grid is significant (an approx-
 imately 20% increase), but the even finer g2 grid does not provide
 further improvement. Thus, the 5 km grid is an acceptable com-
 promise for PMP simulation because it does not compromise sim-
 ulation quality at the expense of reduced computational burden. In
 terms of microphysics schemes, WSM-5 is best for both the finer
 and coarse grids. In the coarse grid, the KF cumulus scheme is also
 a good choice when combined with the Morrison or new Thomp-
 son cumulus schemes.

Fig. 6 shows the evaluation based on metrics that consider
 multiple aspects of the rainfall simulation quality. Fig. 6(a) shows
 the CSI grades (the higher the better). Any skillful forecast or sim-
 ulation should have greater than 0 grades. Fig. 6(c) shows the GSS
 grades (the higher the better). GSS improves CSI grades by taking
 into account the randomness of the observation, and it also requires
 a positive grade for the simulation to be considered skillful. The
 largest differences come from the choice of the IC/BC data source,
 and it is obvious that WSM-5 is the winning microphysics scheme
 at various grids.

As shown in the previous figures, different metrics usually yield
 differing recommendations. They are helpful for specific purposes,
 but a better metric would be desired to simultaneously evaluate

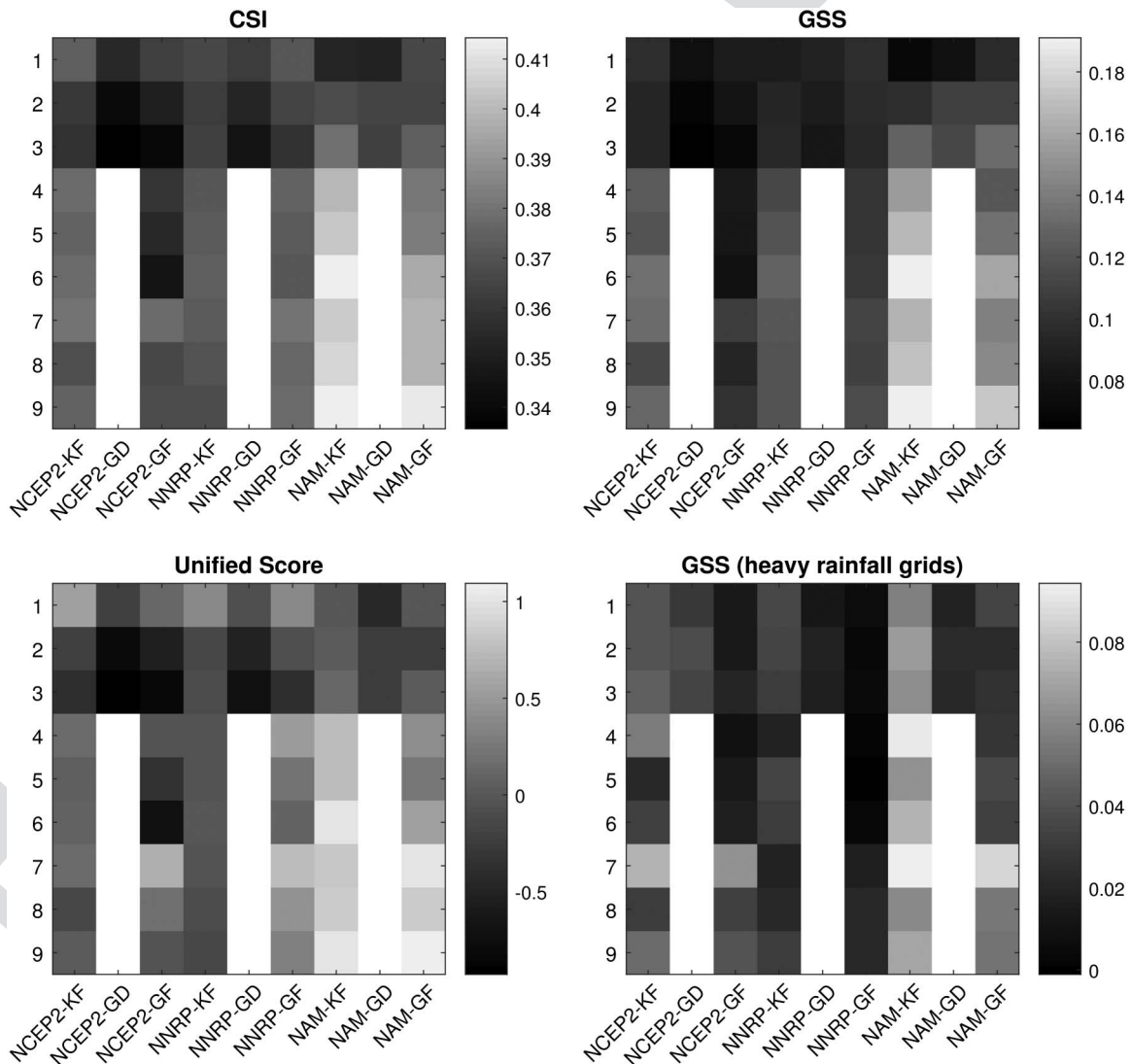


Fig. 6. Evaluation involving multiple aspects of rainfall simulation quality

Table 5. Nash-Sutcliffe Metric between Simulated and Stage IV and Livneh Reference Rainfall Map in the Nashville 2010 Storm Event

T5:2	MP	NCEP2			NNRP			NAM		
		KF	GD	GF	KF	GD	GF	KF	GD	GF
T5:3		15-km grids								
T5:4	Morrison	0.09 (−0.20)	0.05 (−0.04)	−0.03 (−0.09)	−0.03 (−0.43)	0.04 (−0.06)	−0.10 (−0.24)	0.34 (−0.02)	0.17 (−0.08)	0.16 (0.01)
T5:5	Thompson	0.08 (−0.28)	0.09 (−0.01)	0.00 (−0.05)	−0.05 (−0.48)	0.06 (−0.10)	−0.10 (−0.28)	0.36 (0.00)	0.21 (−0.01)	0.21 (−0.01)
T5:6	WSM-5	0.09 (−0.18)	0.08 (−0.09)	0.01 (−0.11)	−0.03 (−0.48)	0.07 (−0.09)	−0.11 (−0.31)	0.33 (−0.01)	0.18 (−0.02)	0.12 (−0.01)
T5:7		5-km grids								
T5:8	Morrison	0.17 (−0.16)	—	−0.09 (−0.46)	−0.02 (−0.38)	—	−0.08 (−0.29)	0.59 (0.43)	—	0.21 (0.01)
T5:9	Thompson	0.00 (−0.69)	—	−0.04 (−0.37)	−0.01 (−0.46)	—	−0.07 (−0.33)	0.48 (0.18)	—	0.22 (0.03)
T5:10	WSM-5	−0.02 (−0.59)	—	−0.05 (−0.51)	0.01 (−0.52)	—	−0.06 (−0.34)	0.48 (0.15)	—	0.26 (0.04)
T5:11		2-km grids								
T5:12	Morrison	0.34 (0.09)	—	0.24 (0.07)	−0.06 (−0.48)	—	−0.06 (−0.48)	0.58 (0.30)	—	0.47 (0.15)
T5:13	Thompson	0.20 (−0.25)	—	0.07 (−0.46)	−0.06 (−0.56)	—	−0.04 (−0.44)	0.47 (0.11)	—	0.38 (−0.05)
T5:14	WSM-5	0.19 (−0.41)	—	0.13 (−0.46)	0.00 (−0.62)	—	−0.01 (−0.51)	0.49 (−0.01)	—	0.36 (−0.20)

Note: Numbers in parentheses are with Livneh reference. Stage IV 48-h total precipitation map is used to evaluate the simulated 48-h total precipitation. Livneh gridded daily precipitation data on May 1, 2010, is used to evaluate the simulated total precipitation on this day.

multiple aspects of the modeling framework. For this purpose, the unified scores [see Eq. (2)] were calculated and are shown in Fig. 6(c). At a coarser grid (15 km), the Morrison microphysics scheme provides the best results. With the NCEP2 IC/BC, the KF scheme yields the highest scores in the g15 domain setup [Fig. 2(a)] group. As the model is run in the finer grids, the NCEP2 results produce lower scores, even negative sometimes. At the finer grids (5 and 2 km), however, NAM yields the best detailed estimates of rainfall. NNRP gives the worst results in both coarse and fine grids, and the scores degrade further in the finer grids. With NAM providing IC/BC, the 2-km simulations are more skillful than the 5-km simulations and less sensitive to the parameterizations used, though the extra improvement is marginal. Also, the GF cumulus scheme produces the best US score in the g5 and g2 domain setups. This implies the GF scheme is scale aware, and it does not double-count the deep convection along with the rainfall that is resolved by the microphysics process.

For extreme events, it is sometimes more useful to analyze the areas with heavy rainfall because they tend to result in the heaviest human and economic losses. NOAA's definition of a heavy storm is an event with an hourly rain rate larger than 7.6 mm. Using this threshold to filter out nonheavy rainfall area, the model performance over the heavy rain area can be evaluated. Fig. 6(d) shows the GSS for the Nashville 2010 event with only heavy (> 7.6 mm/h) rainfall cells and timesteps are treated as rainy cells.

Unlike Fig. 6(b), the KF cumulus scheme tends to work best in the heavy rain area. It is obvious that the KF cumulus scheme is a winning option at various scales. At coarser resolutions, the WSM-5 microphysics scheme tends to work better, whereas Morrison is dominantly better at finer resolutions. The best modeling frameworks recommended by general GSS scores (Fig. 6b) are quite different from those highlighted by the heavy rain-area GSS scores; thus, it is necessary to identify the specific objectives of the modeling framework and choose the corresponding evaluation metrics.

In applications where storm magnitude is important (e.g., when used as input to hydrological or hydraulic models), it is necessary to quantify the simulated rainfall in both spatial extent and amount. Here, the simulated 48-h rainfall maps are compared to Stage IV and Livneh data under Nash-Sutcliffe coefficient. The results are shown in Table 5, where the values in parentheses are the results between the modeled data and the Livneh reference. The higher

the Nash-Sutcliffe coefficient is, the better the model predicts the rainfall pattern. When compared to Stage IV data, Morrison microphysics and KF cumulus schemes outperform others in both coarser and finer grids. The same holds true when they are compared against the Livneh reference, suggesting that their superiority is independent from the choice of reference. In terms of IC/BC, NAM produced the best results, followed by simulations with NCEP2 data.

To check the statistics of simulated rainfall intensity, the hourly rainfall intensities can be plotted as histograms in Fig. 7. In these panels, the *x*-axis shows the hourly rainfall intensity and the *y*-axis shows the total count of such hourly rainfall intensities across the evaluation area in the 48-h duration. Each panel in the figure shows a combination of IC/BC, microphysics, and cumulus schemes. The black lines are the histograms from Stage IV data, the blues lines are those using g15 grids, red lines are those using g5 grids, and green lines are from g2 grids. The biggest difference comes from grid size, where g15 results are often biased away from observation. In most cases, g5 results are closer to the observation, and the improvement from g5 to g2 is not significant. This confirms that g5 is a balance between accuracy and computing burden. Again, Morrison microphysics and the KF cumulus schemes produced better results here.

This evaluation suggests that different demands are best met with different model options for extreme storm simulation. These options have their own strengths and weaknesses. However, collectively, they can be used to generate a multiphysics ensemble forecast, which is useful for providing an “envelope” at a certain confidence level for an engineering application. For example, a range of possible PMP estimates can be much more useful for risk management than a single deterministic value. The results show that the width of the envelope is largely determined by uncertainty in the IC/BCs, followed by sensitivity to grid resolution. The use of the scale-aware GF scheme tends to reduce model sensitivity to resolution as intended and consistently yields high unified scores regardless of the microphysics parameterizations used. These results demonstrate the possibilities of capturing the full range of the envelope using fewer but carefully tested configurations of the end members for design PMP estimates.

In summary, NAM is better for finer-grid simulation, whereas NCEP2 is also a good choice at coarser grids for extreme storms. At finer grids, Morrison or WSM-5 is often a winning option. At the coarse grid scale, the results from different microphysics and

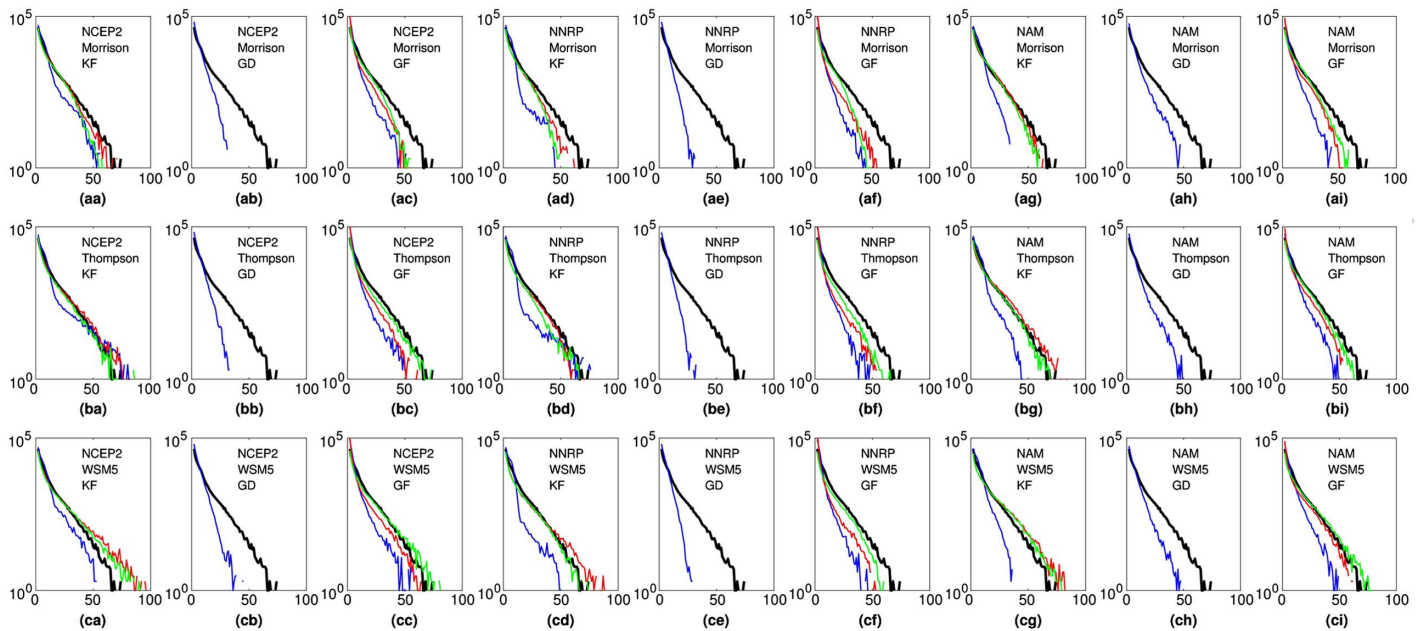


Fig. 7. Evaluation of hourly rainfall intensity histogram simulated by WRF

F7:1

620 cumulus schemes are mixed. Combinations that better resolve the
 621 spatial-temporal structure of the storm are: g15-NAM-Morrison-
 622 KF, g5-NAM-Morrison-KF, g15-NCEP2-Thompson-GF, and g5-
 623 NAM-WSM5 (with KF or GF cumulus parameterization scheme).
 624 The improvement from g5-NAM-WSM5 to g2-NAM-WSM5 is
 625 insignificant (e.g., CSI changed from 0.40 to 0.41), so given the
 626 larger computing requirements, the g2 option is not recommended
 627 here. For general purposes, NAM-Morrison-KF is recommended as
 628 a starting choice. With enough computing capacity, the g5 grid is
 629 recommended, but g15 is also acceptable when running with this
 630 configuration.

631 For the Nashville 2010 storm reconstruction, the recommenda-
 632 tion emerging from the application of the framework differs from
 633 previous studies. For example, Mahoney (2013) recommended the
 634 4 km–1.3 km nested grids, and the NAM forecast IC/BC with the
 635 new Thompson microphysics and no cumulus schemes. The maxi-
 636 mum 48-h total rainfall captured by Mahoney (2013) was
 637 260 mm, whereas in this study, it is 239 mm from the 1.6 km grid.
 638 However, the WSM-5 scheme was not tested by Mahoney (2013).
 639 In this study, the 300-mm 48-h total rainfall isohyet was captured
 640 by using the WSM-5 microphysics scheme. Although these
 641 estimates are smaller than the maximum 48-h total rainfall from
 642 the Stage IV reference precipitation data (330 mm), the use of
 643 WSM-5 represents an advance in capturing the high-precipitation
 644 area.

645 This study includes the four major factors that affect atmos-
 646 pheric model performance. However, there are still some other fac-
 647 tors that can be fine-tuned as needed, such as land surface process,
 648 planetary boundary scheme, and land use condition. Following the
 649 same methodology outlined in this study, these factors can be added
 650 into this evaluation framework to achieve even better simulation
 651 quality, if desired by the engineering community.

652 Validation of Optimal Model Configuration

653 This study proved that the recommended model configuration is
 654 independent from reference choice. The representativeness of this
 655 finding for other storms remains a question. Therefore, the optimal

656 WRF configuration was applied to other two storm events, the 1997
 657 January 1–3 storm in the American River watershed, California
 658 (denoted as the 1997CA event), and the 1980 December 24–26
 659 storm in the Pacific Northwest region (1980PNW event). Because
 660 of data availability, these two events are reconstructed using the
 661 NCEP2 IC/BC.

662 The 1997CA event happened in northern California and caused
 663 a severe flood in Sacramento in the following days. The observed
 664 maximum 24-h precipitation was 284 mm, which made it one
 665 of the greatest storms in this area. The 1980PNW event happened
 666 in the Washington and Oregon, and the observed maximum
 667 24-h precipitation was 234 mm. This storm is one of the big
 668 storms used in the HMR for PMP in the Pacific Northwest region
 669 (HMR57).

670 These storm events were reconstructed using the optimal model
 671 configuration (15 km–5 km nested grids, Morrison microphysics,
 672 and KF cumulus schemes) that was obtained through the Nashville
 673 2010 study. The simulated 3-day total rainfall of these two events,
 674 plus the simulated 1-day rainfall of the Nashville 2010 event,
 675 are shown in Fig. 8. Figs. 8(a and c) show the model reconstructed
 676 3-day precipitation, and Figs. 8(b and d) show the Livneh refer-
 677 ence. The third column shows the difference as WRF-Livneh. It
 678 shows that this model configuration depicts the heavy rainy area
 679 in both spatial extent and magnitude: In the 1997CA simulation,
 680 the model captures the storm center along the Sierra Nevada; in the
 681 1980PNW simulation, it captures the heavy rainy band along the
 682 coast.

683 To quantify the performance of these reconstructions, all nine
 684 model configurations in 15-km grids, and six configurations in
 685 15 km–5 km grids were also tested. The evaluation of the Nash-
 686 Sutcliffe coefficient on the simulated maximum 3-day rainfall is
 687 shown in Table 6. In the 1997CA simulations, this optimal confi-
 688 guration (based on the Nashville 2010 storm) produced the best result.
 689 In the 1980PNW simulations, the performance of this optimal
 690 model configuration is within the top three among all the experi-
 691 ments. This confirms the capability of the optimal model confi-
 692 guration in reconstructing other severe storms, and this is independent
 693 of the choice of reference data.

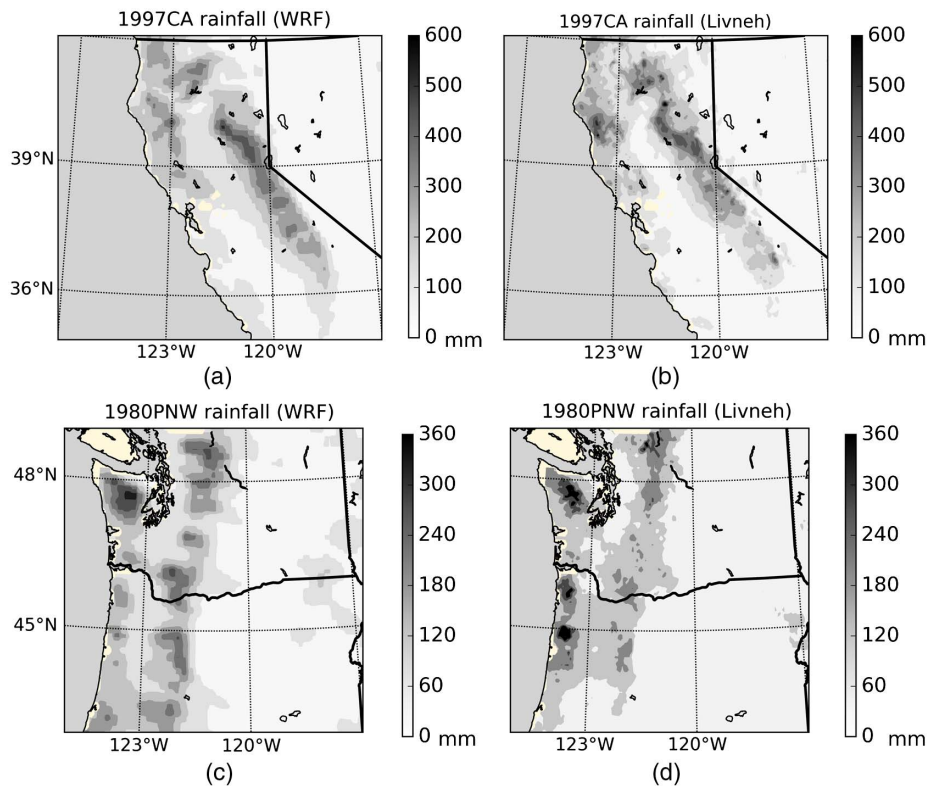


Fig. 8. Evaluation of 1997CA and 1980PNW storms using optimal WRF configuration

Table 6. Nash-Sutcliffe Metric between Simulated and Livneh Reference 3-Day Cumulative Rainfall Map in the 1997CA and 1980PNW Storm Events

	MP	1997CA			1980PNW		
		KF	GD	GF	KF	GD	GF
T6:2							
T6:3	15-km grids						
T6:4	Morrison	0.69	0.67	0.69	0.53	0.54	0.52
T6:5	Thompson	0.61	0.59	0.62	0.50	0.50	0.50
T6:6	WSM-5	0.59	0.57	0.63	0.41	0.41	0.40
T6:7	5-km grids						
T6:8	Morrison	0.64	—	0.68	0.49	—	0.49
T6:9	Thompson	0.57	—	0.63	0.46	—	0.47
T6:10	WSM-5	0.52	—	0.61	0.31	—	0.33

Note: Livneh gridded precipitation data is used as references.

694 Conclusions

695 In this study, an approach to establishing an optimal WRF-based
 696 framework for extreme storm event simulation was investigated.
 697 The goal was to introduce a more physically based method to
 698 the engineering design and analyses community currently engaged
 699 in large water-management infrastructure issues of today and to-
 700 morrow. This framework takes into consideration the uncertainties
 701 coming from various IC/BC data sources, grid resolutions, cloud
 702 microphysics, and cumulus parameterization schemes. These are
 703 the major contributors to the final model performance.

704 In the demonstration, a WRF-based modeling framework was
 705 established for extreme storm events in the CONUS region based
 706 on the Nashville 2010 storm and validated it using two other storms
 707 in California and the Pacific Northwest. Based on the engineering
 708 intent, the best model configuration can be different. For general
 709 purposes, it is recommended that the WRF model be configured

as: 15 km or nested 15 km–5 km grids, the NCEP2 or NAM bound-
 ary condition, and the Morrison microphysics scheme with the
 Kain-Fritsch cumulus scheme. This configuration is either the
 optimal configuration or a starting point that leads to quick conver-
 gence to the final optimal configuration.

For future studies, the authors hope to complete application and
 validation of the optimal WRF modeling framework for a large
 number of storms that were maximized for PMP estimation in
 HMR reports. Because the use of atmospheric numerical models
 for engineering infrastructure analyses is gaining popularity among
 the infrastructure community, future studies should focus on im-
 proving current design and practice among engineers. Some exam-
 ples are: (1) exploration of physics-based probable maximum flood
 (PMF, the flood due to PMP), (2) impact of land use and land cover
 change and global warming on PMP and PMF during extreme
 storms, (3) improving streamflow forecast and thus improving res-
 ervoir and dam operation during extreme storm events, (4) multi-
 physics ensemble-based analyses of numerical model output for
 risk management.

Acknowledgments

This study is motivated by an American Society of Civil Engineers
 (ASCE) Task Committee on “Infrastructure Impacts of Landscape-
 driven Weather change” chaired by the second author. Therein,
 model-based PMPs are currently being explored for modernizing
 current engineering practice of PMPs based on storms many
 decades old. The first author was supported by NASA grant
 NNAX15AC63G. Dr. Ruby Leung acknowledges the support from
 the U.S. Department of Energy Office of Science Biological and
 Environmental Research as part of the Regional and Global
 Climate Modeling Program. The Pacific Northwest National

740 Laboratory is operated for DOE by Battelle Memorial Institute
741 under Contract DE-AC05-76RLO1830.

742 References

743 Abbs, D. J. (1999). "A numerical modeling study to investigate the assump-
744 tions used in the calculation of probable maximum precipitation." *Water*
745 *Resour. Res.*, 35(3), 785–796.
746 Bennett, N. D., et al. (2013). "Characterising performance of environmental
747 6 models." *Environ. Modell. Software*, 40, 1–20.
748 Casagli, N., Dapporto, S., Ibsen, M. L., Tofani, V., and Vannocci, P. (2006).
749 "Analysis of the landslide triggering mechanism during the storm of
750 20th–21st November 2000, in Northern Tuscany." *Landslides*, 3(1),
751 13–21.
752 Chang, H. I., Kumar, A., Niyogi, D., Mohanty, U. C., Chen, F., and Dudhia,
753 J. (2009). "The role of land surface processes on the mesoscale simu-
754 lation of the July 26, 2005 heavy rain event over Mumbai, India." *Global Planetary Change*, 67(1), 87–103.
755 Chen, X., and Hossain, F. (2016). "Revisiting extreme storms of the past
756 100 years for future safety of large water management infrastructures." *Earth's Future*, 4(7), 306–322.
757 Cong, X., Ni, G., Hui, S., Tian, F., and Zhang, T. (2006). "Simulative analy-
758 sis on storm flood in typical urban region of Beijing based on SWMM." *Water Resour. Hydropower Eng.*, 4, 64–67.
759 861 7
762 Del Genio, A. D., Kovari, W., Yao, M. S., and Jonas, J. (2005). "Cumulus
763 microphysics and climate sensitivity." *J. Clim.*, 18(13), 2376–2387.
764 Durkee, J. D., et al. (2012). "A synoptic perspective of the record 1–2
765 May 2010 mid-south heavy precipitation event." *Bull. Am. Meteorol.*
766 *Soc.*, 93(5), 611–620.
767 Evans, J. E., Mackey, S. D., Gottgens, J. F., and Gill, W. M. (2000).
768 9 "Lessons from a dam failure." *Ohio J. Sci.*, 100(5), 121–131.
769 Giannaros, T. M., Kotroni, V., and Lagouvardos, K. (2016). "WRF-
770 LTNGDA: A lightning data assimilation technique implemented in
771 the WRF model for improving precipitation forecasts." *Environ.*
772 10 *Modell. Software*, 76, 54–68.
773 Grell, G. A., and Freitas, S. R. (2014). "A scale and aerosol aware stochastic
774 convective parameterization for weather and air quality modeling." *Atmos. Chem. Phys.*, 14(10), 5233–5250.
775 Hershfield, D. M. (1965). "Method for estimating probable maximum rain-
776 fall." *J. Am. Water Works Assoc.*, 57(8), 965–972.
777 11
778 Huschke, R. E. (1959). *Glossary of meteorology*, American Meteorological
779 Society, Boston.
780 Kumar, A., Dudhia, J., Rotunno, R., Niyogi, D., and Mohanty, U. C.
781 (2008). "Analysis of the 26 July 2005 heavy rain event over Mumbai,
782 India using the Weather Research and Forecasting (WRF) model." *Q. J. R. Meteorol. Soc.*, 134(636), 1897–1910.
783 Kunkel, K. E., et al. (2013). "Probable maximum precipitation and climate
784 change." *Geophys. Res. Lett.*, 40(7), 1402–1408.
785 Laprise, R. (1992). "The Euler equations of motion with hydrostatic
786 pressure as an independent variable." *Monthly Weather Rev.*, 120(1),
787 197–207.
788 Liu, J., Bray, M., and Han, D. (2012). "Sensitivity of the weather research
789 and forecasting (WRF) model to downscaling ratios and storm types in
790 rainfall simulation." *Hydrol. Process.*, 26(20), 3012–3031.

Livneh, B., et al. (2013). "A long-term hydrologically based dataset of land
792 surface fluxes and states for the conterminous United States: Update
793 and extensions." *J. Clim.*, 26(23), 9384–9392.
794 Mahoney, K. (2013). "The impact of model physics and upstream moisture
795 sources on the May 2010 Tennessee flooding event: An examination of
796 precipitation and surface hydrology." 1297
798 Moore, B. J., Neiman, P. J., Ralph, F. M., and Barthold, F. E. (2012).
799 "Physical processes associated with heavy flooding rainfall in Nash-
800 ville, Tennessee, and vicinity during 1–2 May 2010: The role of an
801 atmospheric river and mesoscale convective systems." *Monthly Weather*
802 *Rev.*, 140(2), 358–378.
803 Morrison, H., Thompson, G., and Tatarskii, V. (2009). "Impact of cloud
804 microphysics on the development of trailing stratiform precipitation
805 in a simulated squall line: Comparison of one- and two-moment
806 schemes." *Monthly Weather Rev.*, 137(3), 991–1007.
807 Pennelly, C., Reuter, G., and Flesch, T. (2014). "Verification of the WRF
808 model for simulating heavy precipitation in Alberta." *Atmos. Res.*,
809 135–136, 172–192. 1309
810 Rajeevan, M., Kesarkar, A., Thampi, S. B., Rao, T. N., Radhakrishna, B.,
811 and Rajasekhar, M. (2010). "Sensitivity of WRF cloud microphysics to
812 simulations of a severe thunderstorm event over Southeast India." *Ann.*
813 *Geophys.*, 28(2), 603–619.
814 Rao, Y. V. R., Hatwar, H. R., Salah, A. K., and Sudhakar, Y. (2007).
815 "An experiment using the high resolution ETA and WRF models to
816 forecast heavy precipitation over India." *Pure Appl. Geophys.*,
817 164(8-9), 1593–1615. 1417
818 Sikder, S., and Hossain, F. (2016). "Assessment of the weather research and
819 forecasting model generalized parameterization schemes for advance-
820 ment of precipitation forecasting in monsoon-driven river basins." *J. Adv. Model. Earth Syst.*, 8(3), 1210–1228.
821 Skamarock, W. C., et al. (2008). "A description of the advanced research
822 WRF version 3. NCAR Tech. Note." Tech Report. 1523
824 Stensrud, D. J. (2009). *Parameterization schemes: keys to understanding*
825 *numerical weather prediction models*, Cambridge University Press,
826 Cambridge, UK.
827 Stratz, S. A., and Hossain, F. (2014). "Probable maximum precipitation in a
828 changing climate : Implications for dam design." *J. Hydrol. Eng.*, 10
829 .1061/(ASCE)HE.1943-5584.0001021, 6014006. 1629
830 Tan, E. (2010). "Development of a methodology for probable maximum
831 precipitation estimation over the American River watershed using
832 the WRF model." Univ. of California, Davis, CA.
833 Vaidya, S. S., and Kulkarni, J. R. (2007). "Simulation of heavy precipita-
834 tion over Santacruz, Mumbai on 26 July 2005, using mesoscale model." *Meteorol. Atmos. Phys.*, 98(1-2), 55–66.
835 Winters, A. C., and Martin, J. E. (2014). "The role of a polar/subtropical jet
836 superposition in the May 2010 Nashville flood." *Weather Forecasting*,
837 29(4), 954–974.
838 WMO (World Meteorological Organization). (1986). "Manual for estima-
839 tion of probable maximum precipitation." *Operational Hydrology*
840 *Rep. 1*. 1741
842 Zhang, G. J., and McFarlane, N. A. (1995). "Sensitivity of climate
843 simulations to the parameterization of cumulus convection in the
844 Canadian climate centre general circulation model." *Atmos.-Ocean*,
845 33(3), 407–446.